



# Field emission scanning electron microscopic, X-ray diffraction and ultraviolet spectroscopic analysis of *Terminalia bellerica* based silver nanoparticles and evaluation of their antioxidant, catalytic and antibacterial activity

Kavita Singh<sup>\*</sup>, Vinita Gupta

Agra College, Agra, Affiliated to Dr. Bhimrao Ambedkar University Agra, India

## ARTICLE INFO

### Keywords:

Gallic acid  
2,2-Diphenylpicrylhydrazyl  
HPTLC  
Bragg's Law  
Particle size calculation

## ABSTRACT

In recent years, scientists have come up with ways to make nanoparticles that are inexpensive and good for the environment. *Terminalia bellerica*-based silver nanoparticles (TBAgNPs) were made in this study using methanol extract from *T. bellerica* fruits. This method was quick, economical, and good for the environment. The biosynthesized TBAgNPs were used as antioxidants, antibacterial agents, and anti-catalytic agents. Analytical techniques like XRD, FESEM, and UV-Vis were used to find out more about the spherical TBAgNPs that were made. Also, Cefotaxime-resistant bacteria found in hospitals were used to test how well the TBAgNPs killed bacteria. With the Bauer-agar Kirby's gel diffusion and Mueller-Hinton broth methods, the ability of the synthesized TBAgNPs to stop bacterial growth was tested. After the TBAgNPs were studied, it was found that the average size of their crystals was between 10 and 25 nm. 2,2-Diphenyl-1-picrylhydrazyl (DPPH) reducing tests showed that these AgNPs could act as antioxidants, and TBAgNPs (%inhibition = 20.90% to 94.94%) were better antioxidant than ascorbic acid (%inhibition = 13.80% to 86.10%) and extract (%inhibition = 16.90% to 80.50%). The reduction of methylene blue (MB) to leucomethylene blue (LMB) with sodium borohydride (NaBH<sub>4</sub>) was used as a model to test the catalytic potential of TBAgNPs. On UV spectroscopic analysis at room temperature, TBAgNPs at different concentrations were able to reduce methylene blue effectively. For *Escherichia coli* and *Klebsiella pneumoniae*, the minimum inhibitory concentration (MIC) for TBAgNPs was 0.625 µg/mL and 1.25 µg/mL, respectively. Based on these results, silver nanoparticles made with *Terminalia bellerica* extract may have much biological importance and could be used in making useful therapeutic applications.

## 1. Introduction

Gold, Silver, Platinum, and other precious metal nanoparticles are used in several goods of daily life purposes. Additionally, these metals nanoparticles can be used in a wide range of therapeutic and industrial settings [1]. Nanoparticles have been studied extensively in recent years, and developed various ways of producing them that are cost-effective and safe for the environment. Plant extracts may be superior to other biological agents since they do not necessitate complicated processes and may be utilised in

<sup>\*</sup> Corresponding author.

E-mail address: [kavita.rama.singh@gmail.com](mailto:kavita.rama.singh@gmail.com) (K. Singh).

<https://doi.org/10.1016/j.heliyon.2023.e16944>

Received 12 March 2023; Received in revised form 30 May 2023; Accepted 1 June 2023

Available online 3 June 2023

2405-8440/© 2023 The Authors. Published by Elsevier Ltd. This is an open access article under the CC BY-NC-ND license (<http://creativecommons.org/licenses/by-nc-nd/4.0/>).

large-scale synthesis with little effort on the part of the researcher [2].

Nanoparticle synthesis method should be having minimum or no impact on environment, economically cheaper, easier to make, and highly reproducible. Despite its inaccuracies the biological method yields high-quality nanoscale materials with the desired properties and a harmonious crystal structure. Among biological methods, production of metallic nanoparticles and detoxifying uses, plants have been proved to be a more ecologically acceptable solution [3,4]. The plant extracts are considered superior to other biological agents because of two main reasons. Phytochemicals, such as phenols, flavonoids, ascorbic acid etc., are responsible for the reduction of metal ions to nanoparticles and also help to protect plants against a wide range of pathological illnesses. Synthesizing nanoparticles in an environmentally responsible way is called "green synthesis" [5–10]. This is because there is a possibility that the chemical production of Nanoparticles (NPs) would have negative ecological repercussions. Plants, algae, fungi, and bacteria are increasingly being used in the biological generation of NPs [6]. In the field of synthesis based on microorganisms, fungi are favoured over bacteria species due to the accumulating characteristics of fungus for metals and their higher tolerance. Similarly, a variety of advantages can be gained when plants are used in biological synthesis instead of microbes to produce organic chemicals [11–14].

Nanoparticles made from zinc [15,16], iron [17], and copper oxide (all derived from *Terminalia bellerica* fruit aqueous extract) are effective biological and pharmacological agents against a wide range of disorders [15]. *Terminalia bellerica*, a member of the family Combretaceae, is a large, deciduous tree is commonly grown in India and other parts of South and Southeast Asia [18]. Commonly known as "Baheda", "Beleric" and "Myrobalan", fruit is an important component of Triphala, a classic Ayurvedic medicine. *T. bellerica* has a wide variety of medical uses, including but not limited to the treatment of gastrointestinal and respiratory disorders, liver protection and cholesterol reduction [18]. Its antioxidant activity and capability of decreasing the quantity of sugar in meals like glucose and related compounds is due to presence of polyphenolic molecules such as gallic acid, tannins, and flavones [19]. So, this plant is used to create silver nanoparticles (AgNPs). Many researcher mentioned that ascorbic acid and gallic acid are two of the most active components for reducing the silver salts ( $\text{AgNO}_3$ ) and stabilizing the nanoparticles [20,21]. The phenolic gallic acid concentration is responsible for the redox reduction of metal ions. Gallic acid's hydroxyl groups allow it to convert metal ions into metal nanoparticles [22]. The increased amount of gallic acid aids in the production of smaller nanoparticles because of its enhanced capping ability [23–26]. The presence of several phytochemicals in plant extracts gives them the capacity to function as both a reducing metal ions to their non-valent state and stabilizing agent [11].

Green synthesized AgNPs based on *Terminalia bellerica* were tested in the current work to establish their potential variation in antioxidant, antibacterial activity, and catalytic behaviour when compared NPs' shape, size and surface-area-to-volume ratio. In the present study we were evaluated quality of plant extract based on presence of phytochemicals and antibacterial activity; and to evaluate the antibacterial, antioxidant, and catalytic activity of the *Terminalia bellerica*-based silver nanoparticles (TBAgNPs).

## 2. Materials and methods

### 2.1. Procurement of materials

For present study, *T. bellerica* extract and its principal medicinal molecules i.e. Gallic acid and Ascorbic Acid were chosen for silver nanoparticle production. We purchased Gallic Acid and Ascorbic Acid from Titan Biotech India. The plants fruits were bought at a nearby market and taken to the Botany Department of Dr. Bhimrao Ambedkar University in Agra, India, to have their identities confirmed.

### 2.2. Preparation of plant extract

Dirt and dust were removed from *Terminalia bellerica* fruits by thoroughly rinsing with tap water and then washing with distilled water. After drying in shade for 24hr, the plant components were crushed and blended together to make a fine and coarse powder before being stored at room temperature till further use. The plant powder (30-40 gm) packed in thimble (made by Whatman filter paper No. 01) was then put in a Soxhlet apparatus containing methanol for 25 to 30 cycles in order to get an extract. The soxhlet was heated to between 60 and 70° Celsius, which is the boiling point of methanol. To get the percentage yield of an extract, just divide the dry extract weight by the dry plant powder weight and multiply the result by 100.

### 2.3. Qualitative estimation of phytochemical using biochemical assays

Qualitative phytochemical screening experiments were conducted in order to identify bioactive components present in extract. Plant extract was subjected to screening assays to determine the presence of phyto-constituents such as terpenoids, tannins, saponins, coumarins, quinines, phenol, carbohydrates, glycosides, and steroids. Roy et al. [27] made reference to the applied detailed protocols.

Terpenoids presence was tested by using the Salkowski test: 5 mL extract + 2 mL chloroform were placed over the 3 mL pure  $\text{H}_2\text{SO}_4$ . A reddish-brown interface indicate terpenoid positive sample.

Tannins was present in sample if on treating the 3 mL filtrate (from 0.5 g extract boiled in 20 mL water) with few drops of 0.1% ferric chloride gives a brownish green or blue-black colour.

Saponins emerge frothing in sample on shaking vigorously.

On mixing an equivalent vol/vol proportion of extract and 10%NaOH produces a yellow tint if sample was positive for coumarins.

The presence of quinines is indicated by a blue-green or reddish hue when the plant extract was diluted with 1 mL of concentrated  $\text{H}_2\text{SO}_4$ .

The phenol positive sample develop dark green colour on mixing 1 mL extract + few drops of ferric chloride in the test tube.

Carbohydrates positive sample on having a reducing sugars shown green, yellow, or red in test tube filled with the 1 mL extract +1 mL of Fehling's Reagent. Other test tube served as a control by holding glucose +1 mL of Fehling's Reagent.

To examine the glycosides in the sample, the Keller-Kiliani test was used. Approximately 1 mL of extract plus 1 mL of glacial acetic acid in solution with 1 drop of ferric chloride solution placed above 1 mL concentrated H<sub>2</sub>SO<sub>4</sub>. The presence of glycosides is shown by a brown ring at the interface.

Steroids were tested by putting 0.5 g of methanolic extracts +2 mL of acetic anhydride in a test-tube having 2 mL of H<sub>2</sub>SO<sub>4</sub>. The presence of steroids was identified by a colour changing from violet to blue or green.

#### 2.4. High-performance thin-layer chromatography (HPTLC) analysis of extract

With the assistance of an ATS-4 applicator that was linked to a CAMAG HPTLC system, the extract (10 µL) was disseminated into the pattern of an 8 mm band, 15 mm from the bottom of a 10 × 10 cm pre-activated aluminium supported pre-coated silica gel plate. To a distance of 8 cm, the plate was developed in a pre-saturated twin trough chamber with the mobile phase consisting of Toluene:Ethyl Acetate:Formic Acid (5:4:3, v/v), and it was dried for 5 min in ambient air. Under ultraviolet (UV) light of two different wavelengths, 254 nm and 366 nm, photographs of the developed plate were taken.

#### 2.5. Green synthesis of silver nanoparticle

A fresh solution of silver nitrate in distilled water (1 mM) was prepared for the synthesis of silver nanoparticles. After that 10 mL aqueous plant extract added with 100 mL of 1 mM silver nitrate solution and then the combination was incubated for 15 min at 60°C-80 °C. The solution was incubated at room temperature for 24hrs and then centrifuged at 12000×g for 20 min. The appearance of brown colour supernatant was anticipated to be the outcome of the formation of silver nanoparticles, which would be confirmed by spectrophotometric testing in the UV-visible spectrum. The silver nanoparticles were thoroughly washed in distilled water two to three times before drying in a hot air oven. The nanoparticles that were created were stored at 4 °C in refrigerator (Samsung India Pvt Ltd) till further use [28].

In order to calculate the percentage of AgNO<sub>3</sub> that was converted to AgNP, 10 mL of sterile AgNP suspension were washed and allowed to dry. The percentage conversion efficiency (CE) was determined by weighing dried pellete using the following formula:

The CE is determined by dividing the amount of AgNPs by the amount of AgNO<sub>3</sub>, then multiplying the result by 100. The "AgNPs" value represents the mass of the AgNPs synthesized, whereas the "AgNO<sub>3</sub>" value represents the mass of the Ag<sup>+</sup> ions.

#### 2.6. Synthesis optimization

UV-Visible spectroscopy of the nanoparticle solution was performed at various time intervals, including 30 min, 3 h to 4 h and next day (i.e. 24hrs) using a UV-Vis Spectrophotometer [29]. The biogenic generation of nanoparticles is known to be influenced by pH, temperature and plant extract concentration. The following criteria were evaluated in order to generate the most efficient nanoparticle manufacturing. An increasing concentration (i.e. 10 mL, 20 mL, 30 mL, 40 mL) of *Terminalia bellerica* extract was investigated in 100 mL silver nitrate solution for TBAgNPs formation. The effect of pH on nanoparticle formation was examined by keeping the pH of a silver nitrate-extract combination at 6, 7 and 8 using 0.1 N HCl or 0.1 N NaOH. *Terminalia bellerica* extract and silver nitrate were combined in a 1:9 ratio and incubated for 24 h at 04, 35, and 65° Celsius to see how temperature affects the synthesis process. Every other parameter was remained at its initial value throughout the solution. Furthermore, after one month, the effects of storing silver nanoparticles at room temperature in both refined and unrefined forms were seen. The collected spectra were re-plotted using Microsoft Excel sheets after completing spectrum scans in the 200–800 nm wavelength range.

#### 2.7. Characterization of silver nanoparticle







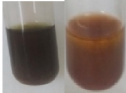


##### 1) UV (UV-vis spectrophotometry)

In order to determine the kinetic behavior of silver nanoparticles based on *T bellerica* (TBAgNPs), an investigation of silver nanoparticles was conducted at wavelengths ranging from 200 to 800 nm using a UV-VIS spectrophotometer (PC-Based Double Beam UV-VIS Spectrophotometer 2202, Systronics India). Distilled water was placed in the reference cuvette next to each cuvette containing an aqueous nanoparticle sample.

##### 2) XRD (X-ray Diffraction)

By employing the X-ray diffraction technique and subjecting the samples to Cu K $\alpha$  radiation, an investigation of the phase evolution and particle size of the samples was carried out. The instructions given in the manual of the instrument were adhered to. An X-ray diffractometer with a wavelength of 0.1540600 nm and a power setting of 40 kV/40 mA (in the 2 $\theta$  range of 20–80) was used to analyse the crystallinity of the synthesize AgNP pellets [30]. The instrument used was a Bruker D8 Advance powder X-ray diffraction (XRD) system. After that, the diffractogram was analysed with the software Origin 6.1, and the average crystalline size was determined by applying the Scherrer formula. This allowed for the calculation of the average crystalline size. With the use of the Scherrer formula, we

**Table 1**  
Phytochemical detection in plant extract.

Phytochemical	Terpenoids	tannins	saponins	cuamrins	quinines	phenol	carbohydrates	glycosides	steroids
Result (all positive test were observed as given herewith)									

can easily determine the particle size:  $D_p = (0.94 \times \lambda) / (\beta \times \cos \theta)$ . Where,  $D_p$  = Average Crystallite size,  $\beta$  = Line broadening in radians i.e. peak Full Width at Half Maximum (FWHM),  $\theta$  = Bragg angle in radians i.e. peak positions,  $\lambda$  = X-Ray wavelength. Typically, instruments are sets with a source made up of copper that produces X Ray wavelength at 0.15418 (Cu K-alpha).  $K$  is the shape factor. X-rays have a wavelength that can range anywhere from 0.01 to 10 nm. When a consequence of this, X-rays are able to readily penetrate the crystal structure of any substance, and as they leave the substance, they expose the properties of that substance. As a consequence of this, X-ray spectroscopy is a very helpful technique that can be used to characterize a wide variety of materials [29].

### 3) FESEM (Field emission Scanning Electron Microscopy) Analysis

The morphological information of all the samples was obtained using FESEM. For FESEM studies, a thin film of AgNPs (1 mg) was created on a carbon tape followed by coating it with platinum. Different magnifications were used to acquire multiple microscopic images. The pictures were taken with a 15 kV Jeol JSM-7610FPlus Field-Emission Scanning Electron Microscope.

### 2.8. Antioxidant activity

The antioxidant activity was checked by 2,2-diphenylpicrylhydrazyl (DPPH) radical scavenging assay. In the assay, 0.1 mM DPPH was reduced with the help of various concentration of TBAGNPs and the TB extracts to evaluate the level of antioxidant activity. The aqueous solution (1 mL) of extract and AgNPs (0.625, 1.25, 2.5, 5.0, and 10  $\mu\text{g}/\text{mL}$ ) were mixed with 3 mL of a methanol and DPPH radicals. After waiting for 30 min, the absorbance was measured at 517 nm. The formula for calculating the percentage of activity that was inhibited was  $[(A_0 - A_1)/A_0]$  multiplied by 100 [31]. (Absorbance without extract is denoted by the symbol  $A_0$ , while absorbance with extract is denoted by  $A_1$ ).

### 2.9. Catalytic activity

The catalytic ability of green synthesized AgNPs was investigated [32] using the reduction reaction of methylene blue by  $\text{NaBH}_4$  as a model reaction [32]. For the purpose of this investigation, methylene blue was obtained from Qualigens Company, India. In order to evaluate the catalytic potential of the TBAGNPs, two reactions were carried out at room temperature in test tubes with a reaction volume of 3.0 mL. In the first reaction, 20 mL of methylene blue at a concentration of one ten-fourth of a million was combined with 2 mL of aqueous fruit extract and 1 mL of water. The reaction was observed for 30 min. During the second reaction, 1 mL of methylene blue at a concentration of  $1 \times 10^{-4}$  M with 1 mL of fresh  $\text{NaBH}_4$  aqueous solution ( $0.1 \text{ molL}^{-1}$ ) was combined with 0.2 mL of extract and 2 mL of TBAGNPs. This reaction was observed after 30 min, 45 min, and 60 min, respectively. The values of the absorption maxima, denoted by the notation  $\lambda_{\text{max}}$ , were evaluated and contrasted with those of methylene blue. The absorbance values were measured using an ultraviolet-visible spectrophotometer.

### 2.10. Antibacterial activity

In order to evaluate the TBAGNPs' potential as antibacterial agents, clinical isolates of bacteria resistant to the antibiotic ciprofloxacin were used. The capacity of the synthesized TBAGNPs to prevent the growth of bacteria was assessed using the Bauer-Kirby's agar gel diffusion method and the Mueller-Hinton broth method. TBAGNPs were tested against *Escherichia coli* and *K. pneumonia* to determine their antibacterial activity. In a previous study (unpublished), these strains were isolated from blood samples and found to possess CTX-M and TEM gene; genes responsible for cefotaxime resistance microbes. The dilution test was carried out so that the minimum inhibitory concentrations (MICs) of TBAGNPs, which were effective in preventing the growth of bacteria, could be determined. The bacteria (*E. coli* and *K. pneumoniae*) were given progressively higher concentrations of crude extracts (ranging from 20 to 200 mg/mL) and TBAGNPs (0.625, 1.25, 2.5, 5.0, and 10  $\mu\text{g}/\text{mL}$ ) as treatments. In addition to this, we made use of a positive control (cefotaxime in a concentration 10  $\mu\text{g}/\text{mL}$ ) as well as a negative control (treatment with no antibiotics). After a period of treatment lasting 24 h, the turbidity of the bacterial suspension was visually evaluated in order to ascertain whether or not the bacteria had multiplied. The minimum inhibitory concentration (MIC) was a lowest concentration of test molecule that was able to stop the visual bacterial growth of bacteria even after 48hrs of culture conditions. Each and every experiment was carried out a total of three times.

## 3. Results

**Yield of extract:** It was discovered that the powdered form of *Terminalia bellirica* produced an extract with a weight of 47.82% (18.41 out of 38.5 gm) when it was subjected to 25 cycles of the Soxhlet apparatus using 350 mL of methanol as the solvent.

**Phytochemical detection:** Terpenoids, tannins, saponins, cuamrins, quinines, phenol, carbohydrates, glycosides, and steroids were all detected in qualitative analyses of the extract (Table 1).

### 3.1. HPTLC analysis

In an HPTLC analysis of methanol solvent extracts, the phenolic profile of *Terminalia bellirica* was determined to be present. The component of gallic acid and ascorbic acid in the sample was analysed using UV light at two different wavelengths (366 and 254 nm), as shown in Fig. 1 a and b. The  $R_f$  values were tallied, and the results are shown in Table 2 that is attached to Fig. 1.

Fig. 1 and Table 2 documented the derivatization with sulfuric acid spray reagent; there were 5 spots under 366 nm and 6 spots under 254 nm. The Rf values indicated the presence of gallic acid and other phenolic compounds in the samples.

### 3.2. AgNPs synthesis and UV analysis

We had found all of the  $\text{Ag}^+$  had changed into AgNPs with *Terminalia bellerica* in around 45 min to 24hrs. The formation of AgNPs occurred promptly at pH 7 following the addition of TB extract, as evidenced by the transformation of the solution from a light yellow hue to a dark brown colour with a prominent absorbance peak located at  $\lambda_{\text{max}}$  420 nm (Fig. 2b). The peak was deviated from signatory peak of 420 nm at higher (400 nm, Fig. 2a) and lower pH (450 nm, Fig. 2c).

The detection of TBAGNPs peaks was unsuccessful at higher extract concentrations (30 mL and 40 mL). A discernible pattern of a steady decline in absorbance was noted at these concentrations. This phenomenon could be ascribed to two possible factors: firstly, the presence of phytochemicals that impede the reduction reaction leading to the non-production of AgNPs; secondly, at higher extract concentrations, the unused extract molecules may have acted as a shield, thereby obstructing the AgNPs' absorbance.

The synthesis of TBAGNPs was not achieved at a temperature of 4° Celsius. The sample exhibited a discernible signature in the form of a peak with a wavelength of 420 nm, which was detected at a temperature of 35 °C following a 24-h duration. Nonetheless, the identical peak was detected in a reduced timeframe of 45 min upon elevating the temperature to 65 °C. According to the results, the phytochemical responsible for reducing  $\text{Ag}^+$  ions displays better efficiency at a particular temperature and may exhibit decreased efficacy at a temperature of 4° Celsius.

In the study the reduction of  $\text{AgNO}_3$  (0.034 gm) to AgNPs (0.021 gm) occurred upon treatment of *Terminalia bellerica* extract in 200 mL of distilled water (solvent), at a temperature of 65° Celsius and a pH of 7. Based on the computation, the yield percent of AgNP is determined to be 61.76% by applying the formula  $((0.021/0.034) \times 100)$ .

An XRD analysis was carried out in order to verify the crystalline structure of produced silver nanoparticles (Fig. 3). The pattern of X-ray diffraction exhibited strong peaks at  $2\theta$  values of 38.02°, 44.16°, 64.30° and 77.29° which were consistent with the values that were recorded in the JCPDS file for Silver: 04–0783. XRD data analysis and peak indexing were carried out, and the results led to the discovery that the above-mentioned  $2\theta$  values correspond to the (111), (200), (220) and (311) planes of Bragg's reflections for face-centered cubic crystallographic planes of silver crystals (Table 3). The findings matched the information contained on JCPDS card file

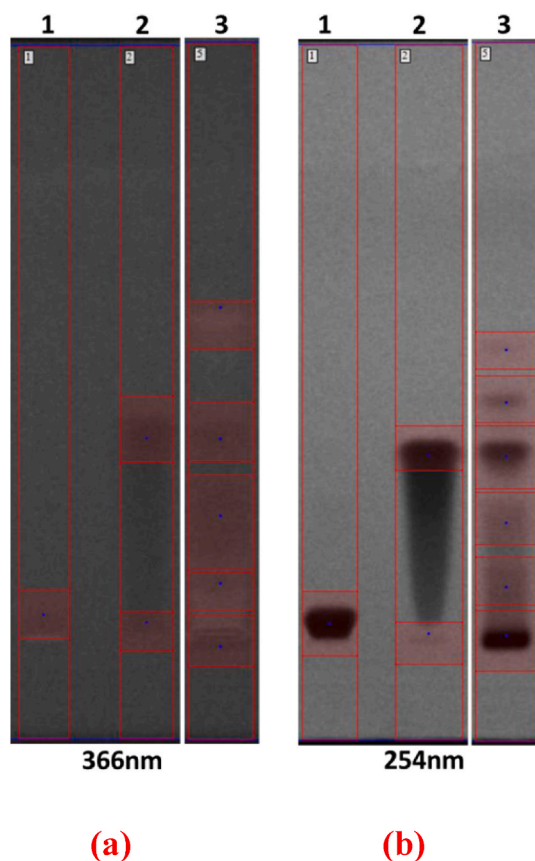


Fig. 1. The graphical representation depicts the separation of phytochemicals based on their Rf values, as observed through the bands visible under 366 and 254 nm wavelengths.

**Table 2**

Represents the numerical values of Rf, area, and volume for bands in each lane can be observed in Fig. 1a and b.

Lane details of Fig. 1a under 366 nm						
ID	Width	Band	Volume	Displayed Volume	Notes	
1	59	1	5289232	52.89	Ascorbic Acid	
2	63	2	6337107	63.37	Gallic Acid	
3	63	5	45027738	450.28	<i>Terminalia bellerica</i>	
Lane-wise band description of Fig. 1a under 366 nm						
Lane ID	Band ID	Rf	Area	Volume	Displayed Volume	Notes
1	1	0.055	3363	5281232	52.89	Ascorbic Acid
2	1	0.392	4851	5423922	54.24	Gallic Acid
	2	0.04	2961	913185	9.13	Gallic Acid
3	1	0.638	3528	1135953	11.36	<i>Terminalia bellerica</i>
	2	0.388	4347	10985814	109.86	
	3	0.243	6993	20632752	206.33	
	4	0.115	2709	3118311	31.18	
	5	0	3780	9154908	91.55	
	6	0.031	5110	66466890	664.67	
Lane details of Fig. 1b under 254 nm						
ID	Width	Band	Volume	Displayed Volume	Notes	
1	63	1	53273619	532.74	Ascorbic Acid	
2	77	2	29267392	292.67	Gallic Acid	
3	70	6	187358850	1873.59	<i>Terminalia bellerica</i>	
Lane-wise band description of Fig. 1b under 254 nm						
Lane ID	Band ID	Rf	Area	Volume	Displayed Volume	Notes
1	1	0.052	4914	53273619	532.74	Ascorbic Acid
2	1	0.386	4158	27203176	272.03	Gallic Acid
	2	0.033	3927	2064216	20.64	Gallic Acid
3	1	0.592	3150	2288230	22.88	<i>Terminalia bellerica</i>
	2	0.489	3920	10893470	108.93	
	3	0.383	5320	43032570	430.33	
	4	0.252	4410	28175700	281.76	
	5	0.126	4060	36501990	365.02	
	6	0.031	5110	66466890	664.67	

no. 01-087-0717 [33]. In addition, using Scherrer's formula [34], we determined that the average size of TBAGNPs was 15.943 nm.

The computation of the interplanar d-spacing was based on Bragg's Law, which was utilised as the foundation for the calculation (Table 3). When the peaks were indexed using the resulting d values, the results that were obtained were equivalent to those that were obtained using the 2 $\theta$ .

The Debye-Scherrer formula was utilised in order to carry out the computation for the particle size (D), as is given in Table 2 and was computed by making use of OriginPro 8.0 to carry out a Gaussian fit to the diffraction peaks. Both of these procedures were carried out in order to determine the particle size. According to the most prominent 111 peak, the size of the particles is measured to be 15.991 nm (Table 3).

### 3.3. FESEM analysis

An investigation on the surface morphology of green-synthesized AgNPs was carried out using FESEM analysis. The production of nanoparticles was demonstrated by the SEM micrograph (Fig. 4 a, b), which displayed almost spherical nanoparticles with a fairly constant particle size up to 20.6 nm with a few occurrences of larger particle size. An in-depth examination of the aggregates revealed that the generated nanoparticles were not in direct physical contact with one another.

### 3.4. DPPH analysis

The findings demonstrated that the antioxidant activity can be contributed to AgNPs, vitamin C, and extract. The antioxidant activity of the AgNPs was verified to be higher than that of vitamin C and *T. bellerica* extract (Fig. 5) respectively. The presence of functional groups on the surface of silver nanoparticles is what causes these characteristics of silver nanoparticles to manifest themselves.

### 3.5. Catalytic activity

In the current investigation, extract and TBAGNPs were utilised as catalysts to degrade, reduce, or oxidise a low concentration of MB



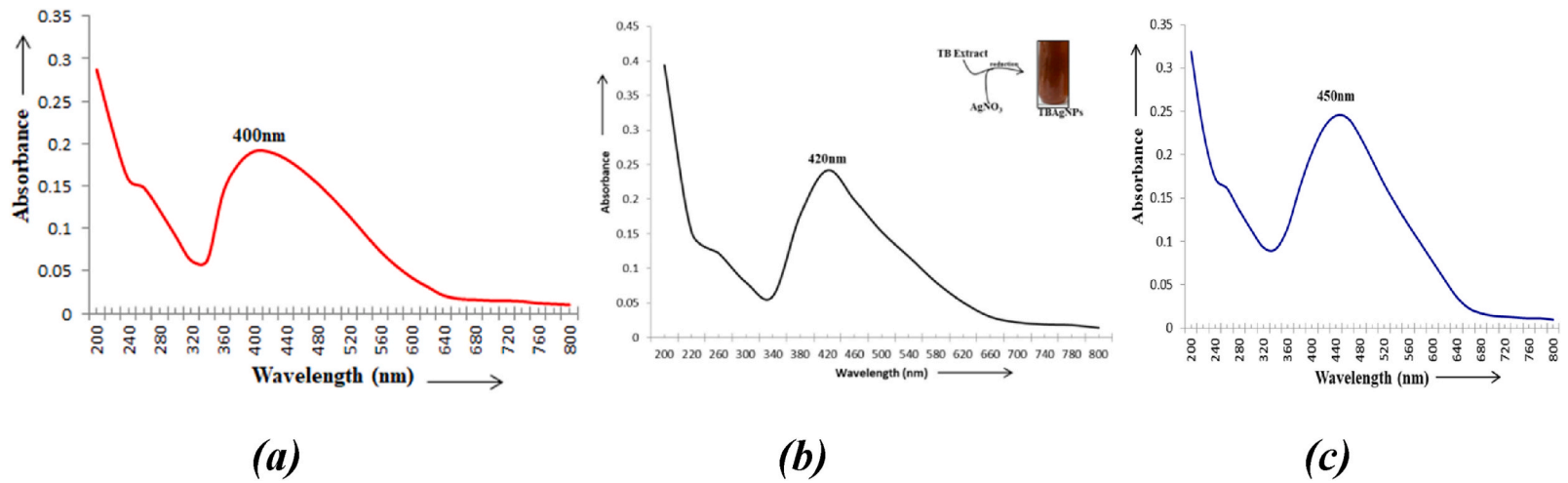


Fig. 2. UV-visible absorption spectra ( $\lambda_{\max}$  vs absorbance) of TBAgNPs at (a)pH8 (b)pH7 and (c)pH6.



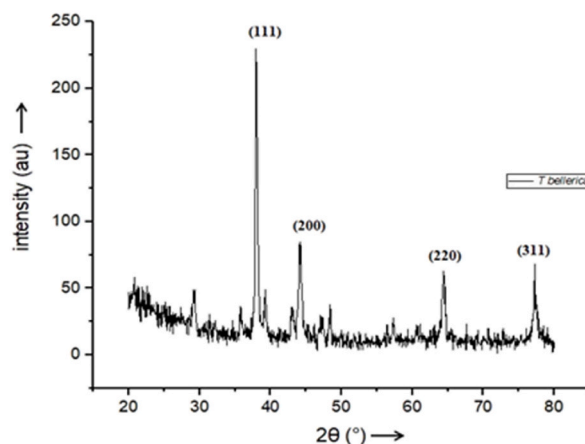


Fig. 3. XRD pattern of TBAGNPs.

Table 3

XRD peak indexing, d-spacing and particle size calculation.

Peak position (2θ)	Sinθ	1000 × Sin <sup>2</sup> θ	1000 × Sin <sup>2</sup> θ/35	hkl	d' = λ/2Sinθ (Å)	d = d' × 10 (nm)	FWHM (beta)	particle size (nm) [D = 0.9 × λ/β cos θ]
38.016	0.325	106	3	111	2.364	0.2364	0.52524	15.991
44.163	0.375	141	4	200	2.048	0.2048	0.81956	10.457
64.302	0.532	283	8	220	1.447	0.1447	0.73254	12.804
77.285	0.625	390	11	311	1.233	0.1233	0.41462	24.522
<b>Average particle size = 15.943 nm</b>								

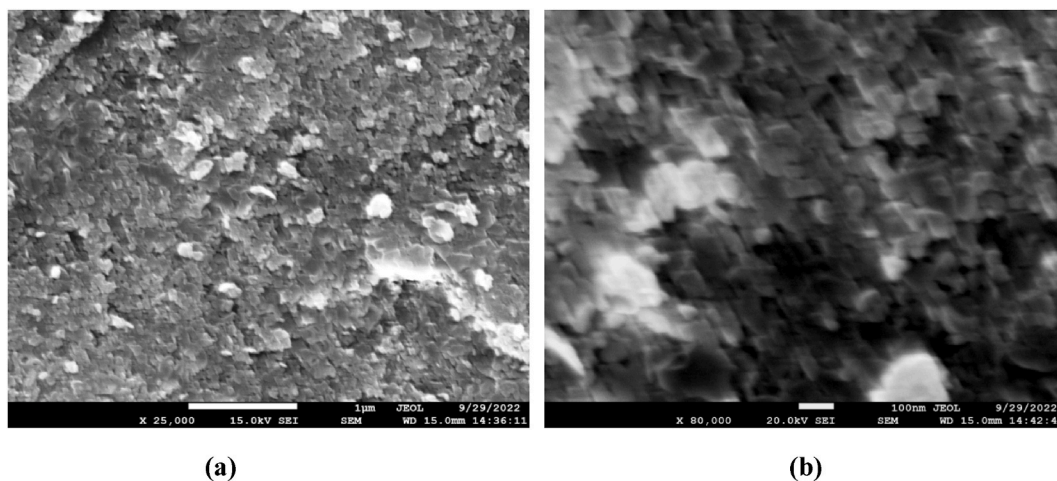


Fig. 4. FESEM pictograph of TBAGNPs captured at magnification (a) 25000x and (b) 80000×

in order to get rid of it. Initially, the silver nanoparticles that had been coated with extracts were utilised as a catalyst in the reduction process of MB that was carried out with NaBH<sub>4</sub>. Following the complete disappearance of the maximum absorption wavelength of MB (max = 660 nm), which does not overlap with the SPR peak of AgNPs at 420 nm, UV-vis spectroscopy is used to investigate the catalytic reduction of MB by using TBAGNPs (Fig. 6). The solution of MB and extract (MB Ex in Fig. 6) yielded a maximum peak at 680 nm. Upon reaction with TBAGNPs, the MB peak was detected at a wavelength of 660 nm after 30 min, and at 620 nm after 45 and 60 min. The peak height at 620 nm exhibited a reduction over time, as evidenced by the comparison between the readings obtained at 45 and 60 min, respectively.

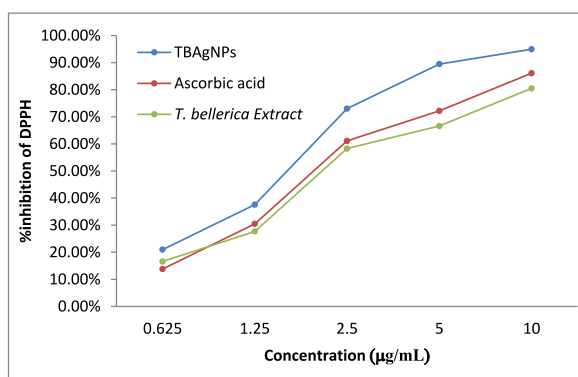


Fig. 5. DPPH Scavenging activity of TBAgNPs, Ascorbic acid and T. bellerica extract.

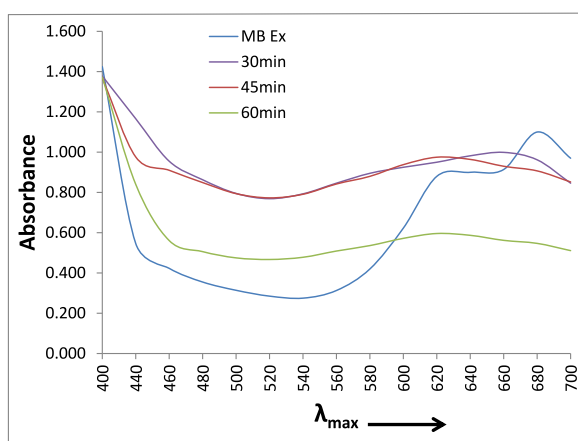


Fig. 6. Catalytic analysis of TBAgNPs by using it in methylene blue reduction reaction. (For interpretation of the references to colour in this figure legend, the reader is referred to the Web version of this article.)

### 3.6. Anti-bacterial activity

TBAgNPs play significant bactericidal effects (Fig. 7, Table 4). TBAgNPs were significantly more successful than the extract in preventing the development of both kinds of bacteria strains.

For *Escherichia coli* and *Klebsiella pneumoniae*, the minimum inhibitory concentration (MIC) for TBAgNPs was 0.625 µg/mL and 1.25 µg/mL, respectively.

## 4. Discussion

Due to their surface plasmon resonance phenomenon (SPR), it was easy to figure out and keep track of how silver nanoparticles were made [35]. It was made abundantly evident that after reduction of  $\text{AgNO}_3$  a dark brown colour and findings of the UV–Vis spectrophotometry indicate the presence of a high peak at 420 nm (therefore we denoted it a signatory peak), which points to the synthesis of AgNPs. This signal was generated as a result of the activation of the plasmon resonance on the surface of the AgNPs. Impurities from bio-extract molecules such as proteins, enzymes, and salts are responsible for peak deviation [36]. SPR is the interaction between electromagnetic radiation and electrons in the conduction band around the nanoparticles [37]. This results in a well-defined absorption band in the visible area, which is an indication of the optical sensitivity of materials with varying scales [38]. Using a UV–Vis spectrophotometer, Shireen et al. [39], analysed various plant-based silver nanoparticles and discovered that the test AgNPs exhibited a difference in their  $\lambda_{\text{max}}$  absorption. It was hypothesised that the differences in sample absorbance were caused by the various phytoingredients that were present in the various extracts and had the potential to active reduction of  $\text{Ag}^{+1}$  to  $\text{Ag}^{\bullet}$ . Literature that was similar to this one also hinted at the abundant presence of polyphenols as the primary molecules lying behind a peak that had greater intensities. Many green synthesis publications credit polyphenols with bringing about the reduction of metal ions to their nanostates. Because the activation of particle surface plasmon resonance causes increased particle shape and size, the peak absorbance measured at a greater intensity may also be responsible for this effect. Ahmad et al. [40], reviewed a variety of spectroscopic features of AgNPs that were manufactured in an environmentally friendly manner. Based on the information that was made available, it was

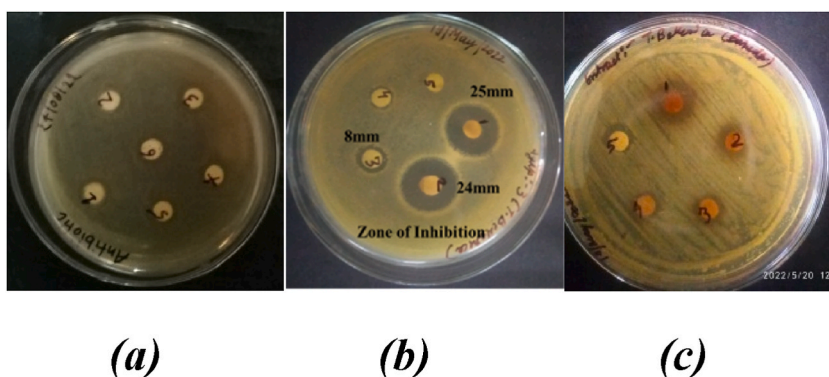


Fig. 7. Inhibition of *Escherichia coli* by (a) cefotaxime (b) TBAgNPs (c) *Terminalia bellerica* plant extract.

**Table 4**  
Antibacterial activity of TBAgNPs against CTX-M positive bacterial strains.

S.No.	Bacterial Strains	Dose of TBAgNPs					MIC
		0.625 µg/mL	1.25 µg/mL	2.5 µg/mL	5.0 µg/mL	10 µg/mL	
1	<i>E. coli</i>	A	A	A	A	A	0.625
2	<i>K. pneumoniae</i>	P	A	A	A	A	1.25

Note: P = growth present ; A = Growth absent



determined through analysis that the region of wavelengths between 350 and 500 nm contains the green AgNPs with the highest peak absorbance. The presence of active polyphenols in plant extracts and the stimulation of reduced silver upon absorbance of UV-Vis rays are responsible for the peak that may be seen between an intensity of 400 and 450. The AgNPs based on the peels of banana, orange, mandarin, and kivi fruit was reported by Abd El-Aziz et al. [41], a colour shifted from yellow to a dark brown with increasing intensity. Within 72 h, a noticeable alteration occurred [41,42]. The size, shape, and yield of synthesized NPs are all affected by the shift in pH, which in turn affects plant metabolism and the plant's capacity to chelate and reduce metal ions. Metabolites found in plants range widely in structure and function. The temperature may also has a similar effect on NP synthesis as well.

The findings of the X-ray diffraction experiment made it abundantly evident that the produced AgNPs had a crystalline structure. There were also a few prominent peaks that could not be recognised, and it is possible that they were caused by certain biomolecules that were involved in the production of nanoparticles. In current work *Terminalia bellerica* was used as a mediator in the synthesis of silver nanoparticles, and identical reflection peaks were found in those nanoparticles.

The production of nanoparticles was demonstrated by the SEM micrograph (Fig. 4), which displayed almost spherical nanoparticles with a fairly constant particle size up to 20.6 nm with a few occurrences of larger particle size. An in-depth examination of the aggregates revealed that the generated nanoparticles were not in direct physical contact with one another. This finding is consistent with the notion that phytoconstituents were responsible for the stabilisation of AgNPs [32,42].

The cationic MB dye is a water-soluble dye that is capable of consuming the oxygen that has been dissolved in water. It was observed that the colour of the MB had changed from blue to colourless. There was no change in the colour of the MB aqueous solution when TBAgNPs were not present, indicating the catalytic performance of TBAgNPs. The intensity of the hue faded down gradually as time passed [43]. The findings of Edison and Sethuraman [44] in the plant-mediated production of silver nanoparticles are quite compatible with these results, which show good agreement with those findings.

The degradation may have been induced by adsorption had taken place on the surfaces of the AgNPs [45]. AgNPs can take on a variety of forms, depending on their magnitude. A large amount of catalytic activity is demonstrated because to such enormous surface-area-to-volume ratio that is exhibited [46–49]. We agree with the assumption given by those researchers, namely that the size of the AgNPs decreases while the number of Ag atoms increases, which makes it simpler to adsorb methylene blue dye onto the surface of the catalyst.

The development of hydroxy radicals (OH) on the surface of the catalyst is strongly connected to the rate of degradation, and the likelihood that these radicals may react with coloured molasses is also directly related to this creation [50,51]. Because the active sites on the photocatalyst surface are also being covered with colour ions and there are fewer photons reaching the photocatalyst surface, the generation of hydroxyl radicals on the surface of the catalyst decreases as the concentration of colour increases. This is the cause of

the slow hydroxyl radicals output [52,53]. In addition, the degradation value has grown when the catalyst is increased to the greater concentration, and the reason for this is that the quantity of adsorptions that are accessible as well as the number of catalysts that are available on a metal-nanoparticle has increased [53,54]. When there is a rise in the concentration of TBAGNPs in the solution, the decolorization rate experiences a decline as a consequence of an increase in the turbidity of the suspension.

Dye degradation is also brought on by an enhanced migration of the holes on the corresponding surface into the surface of the AgNP [55,56]. Since there was a decrease in the available surface area of the metals, the efficiency of the catalyst might be improved by increasing the availability of surface area. A decrease in particle size will result in an increase in catalytic activity; however, if a significant dimension has been reached below, it signals that additional reductions will inhibit the process [57]. Metal nanoparticles provide assistance for the process of transferring electrons from a donor to an acceptor [58]. Silver nanoparticles are susceptible to coagulate and agglomerate, it may make them expensive to use. To minimize the cost of its application, silver could be immobilised on various support materials to remove pollutant dyes from wastewater.

Both selected *Klebsiella pneumoniae* and *Escherichia coli* were having CTXM gene in present study. The CTXM gene is responsible for production of extended spectrum beta lactamase (esbl) enzyme in bacteria to protect themselves from cefotaxime medicine [59]. In present case the size of the TBAGNPs is a factor in the activity. AgNPs with smaller sizes are often more effective because they are able to quickly pass through cellular barriers once they have been absorbed and are then able to impair the physiological activities of the bacterium even in presence of esbl enzyme secretion. Because of their tiny size, bacteria may be able to efficiently bind and take up the substance, which may lead to the bacterium's demise. The precise method by which AgNPs inhibit the growth of bacteria is not yet fully understood. Despite this, a number of studies have shown that the size, shape, concentration, and colloidal state of the AgNPs all play a significant role in determining the bactericidal effects of the particles. Findings suggest they may have potential uses in the field of medicine.

## 5. Conclusions

*Terminalia bellerica* extract is having polyphenols that help synthesize silver nanoparticles (here coded as TBAGNPs). TBAGNPs were potential antioxidant, antibacterial, and catalytic activity may be due to having small (10–25 nm) crystalline sizes. TBAGNPs outperformed ascorbic acid and extract in DPPH assays. TBAGNPs efficiently catalysed methylene blue reduction at room temperature. Due to their size, shape, concentration, and colloidal condition, *Terminalia bellerica* extract-based silver nanoparticles may have benefits.

## Funding

This research did not receive any specific grant from funding agencies in the public, commercial, or not-for-profit sectors.

## Author contribution statement

Kavita Singh: Conceived and designed the experiments; Performed the experiments; Analysed and interpreted the data; Contributed reagents, materials, analysis tools or data; Wrote the paper.

Vinita Gupta: Conceived and designed the experiments; Analysed and interpreted the data; Contributed reagents, materials, analysis tools or data; Wrote the paper.

## Data availability statement

Data included in article/supp. material/referenced in article.

## Declaration of competing interest

The authors declare that they have no known competing financial interests or personal relationships that could have appeared to influence the work reported in this paper.

## Acknowledgment

The Authors are grateful to the teachers and staff of School of Life Sciences, Dr. Bhimrao Ambedkar University Agra, for support the work done in their labs. Authors also acknowledges the Technical team in Dayalbagh Education Institute, Dayalbagh Agra for XRD and FESEM experiments.

## References

- [1] R. Gupta, H. Xie, J. Environ. Pathol. Toxicol. Oncol. 37 (2018) 209–230.
- [2] B. Bhardwaj, P. Singh, A. Kumar, S. Kumar, V. Budhwar, Adv. Pharmaceut. Bull. 10 (2020) 566–576.
- [3] A. Kale, Y. Bao, Z. Zhou, P.E. Prevelige, A. Gupta, Nanotechnology 24 (2013), 045603.
- [4] A.A. Khan, E.K. Fox, M.L. Górzny, E. Nikulina, D.F. Brougham, C. Wege, A.M. Bittner, Langmuir 29 (2013) 2094–2098.
- [5] K.S. Ahmad, S. Yaqoob, M.M. Gul, Rev. Inorg. Chem. 42 (2021) 239–263.

- [6] J. Singh, T. Dutta, K.-H. Kim, M. Rawat, P. Samddar, P. Kumar, J. Nanobiotechnol. 16 (2018).
- [7] M.S.S. Danish, L.L. Estrella-Pajulas, I.M. Alemaida, M.L. Grilli, A. Mikhaylov, T. Senjyu, Metals 12 (2022) 769.
- [8] S.A. Akintelu, A.S. Folorunso, F.A. Folorunso, A.K. Oyebamiji, Heliyon 6 (2020), e04508.
- [9] S. Panhwar, Curr. Anal. Chem. 17 (2021) 1169–1181.
- [10] S.A. Akintelu, A.K. Oyebamiji, S.C. Olugbeko, A.S. Folorunso, Ecletica Quimica Journal 46 (2021) 17–37.
- [11] N. Pantidos, J. Nanomed. Nanotechnol. 5 (2014).
- [12] J.A. Aboyewa, N.R.S. Sibuyi, M. Meyer, O.O. Oguntibeju, Plants 10 (2021) 1929.
- [13] S. Ojha, Biol. Sci. 2 (2022).
- [14] F. Ahmad, N. Ashraf, T. Ashraf, R.-B. Zhou, D.-C. Yin, Appl. Microbiol. Biotechnol. 103 (2019) 2913–2935.
- [15] S.M.H. Akhter, F. Mohammad, S. Ahmad, BioNanoScience 9 (2019) 365–372.
- [16] N. Rana, S. Chand, A.K. Gathania, Int. Nano Lett. 6 (2016) 91–98.
- [17] G.B. Jegadeesan, K. Srimathi, N. Santosh Srinivas, S. Manishkanna, D. Vignesh, Biocatal. Agric. Biotechnol. 21 (2019), 101354.
- [18] A. Gupta, R. Kumar, P. Bhattacharyya, A. Bishayee, A.K. Pandey, Phytomedicine 77 (2020), 153278.
- [19] M.P. Singh, A. Gupta, S.S. Sisodia, J. Compl. Integr. Med. 17 (2019).
- [20] S. Al-Zahrani, S. Astudillo-Calderón, B. Pintos, E. Pérez-Urria, J.A. Manzanera, L. Martín, A. Gomez-Garay, Plants 10 (2021) 1671.
- [21] A. Gibala, P. Żeliszewska, T. Gosiewski, A. Krawczyk, D. Duraczyńska, J. Szaleniec, M. Szaleniec, M. Oćwieja, Biomolecules 11 (2021) 1481.
- [22] X. Liu, J. Wang, Y. Wang, C. Huang, Z. Wang, L. Liu, ACS Omega 6 (2021) 23630–23635.
- [23] P.P. Gan, S.F.Y. Li, Rev. Environ. Sci. Biotechnol. 11 (2012) 169–206.
- [24] V. Pahal, P. Kumar, P. Kumar, V. Kumar, Plant Sci. Today 9 (2022) 345–356.
- [25] R.H. Taha, Inorg. Chem. Commun. 143 (2022), 109610.
- [26] A. Gangula, R. Podila, M. R. L. Karanam, C. Janardhana, A.M. Rao, Langmuir 27 (2011) 15268–15274.
- [27] P. Roy, S. Amdekar, A. Kumar, V. Singh, BMC Compl. Alternative Med. 11 (2011).
- [28] K. Anandalakshmi, J. Venugobal, V. Ramasamy, Appl. Nanosci. 6 (2015) 399–408.
- [29] P. Jamdagni, P. Khatri, J.S. Rana, Adv. Mater. Proceed. 3 (2021) 129–135.
- [30] A. Rautela, J. Rani, M. Debnath, (Das), J. Analy. Sci. Tech. 10 (2019).
- [31] S. El-Newary, A. Ibrahim, M. El-Raey, Egypt. Pharm. J. 16 (2017) 168.
- [32] S. Patil, G. Chaudhari, J. Paradeshi, R. Mahajan, B.L. Chaudhari, 3 Biotech 7 (2017).
- [33] P. Velusamy, C.-H. Su, G. Venkat Kumar, S. Adhikary, K. Pandian, S.C.B. Gopinath, Y. Chen, P. Anbu, PLoS One 11 (2016), e0157612.
- [34] P. Logeswari, S. Silambarasan, J. Abraham, J. Saudi Chem. Soc. 19 (2015) 311–317.
- [35] A.J. Kora, R.B. Sashidhar, J. Arunachalam, Process Biochem. 47 (2012) 1516–1520.
- [36] B. Gurunathan, P.V. Bathrinarayanan, V.K. Muthukumarasamy, D. Thangavelu, Acta Metall. Sin. 27 (2014) 569–572.
- [37] E. Ringe, J.M. McMahon, K. Sohn, C. Cobley, Y. Xia, J. Huang, G.C. Schatz, L.D. Marks, R.P. Van Duyne, J. Phys. Chem. C 114 (2010) 12511–12516.
- [38] C. Noguez, J. Phys. Chem. C 111 (2007) 3806–3819.
- [39] F. Shireen, B. Ahmad, L. Ahmad, S.A. Khan, A. Rauf, A.A. Khalil, A. Zia, Y.N. Mabkhot, Z.M. Almarhoon, M.F. Ramadan, J. Sharifi-Rad, J. Nanomater. 2022 (2022) 1–13.
- [40] B. Ahmad, F. Shireen, A. Rauf, M.A. Shariati, S. Bashir, S. Patel, A. Khan, M. Rebezov, M.U. Khan, M.S. Mubarak, H. Zhang, IET Nanobiotechnol. 15 (2021) 1–18.
- [41] A.R.M. Abd El-Aziz, A. Gurusamy, M.R. Alothman, S.M. Shehata, S.M. Hisham, A.A. Alobathani, Saudi J. Biol. Sci. 28 (2021) 1093–1099.
- [42] A.R. Abd El-Aziz, M.R. Al-Othman, M.A. Mahmoud, Biotechnol. Biotechnol. Equip. 32 (2018) 1174–1182.
- [43] R.M. Kumari, N. Thapa, N. Gupta, A. Kumar, S. Nimesh, Adv. Nat. Sci. Nanosci. Nanotechnol. 7 (2016), 045009.
- [44] T.J.I. Edison, M.G. Sethuraman, Process Biochem. 47 (2012) 1351–1357.
- [45] Y.-H. Kim, E.R. Carraway, Environ. Sci. Technol. 34 (2000) 2014–2017.
- [46] V.K. Vidhu, D. Philip, Micron 56 (2014) 54–62.
- [47] W.A. Shaikh, S. Chakraborty, R. Ul Islam, Desalination Water Treat. 130 (2018) 232–242.
- [48] T.N.J.I. Edison, R. Atchudan, N. Karthik, J. Balaji, D. Xiong, Y.R. Lee, Fuel 280 (2020), 118682.
- [49] G. Ganapathy Selvam, K. Sivakumar, Appl. Nanosci. 5 (2014) 617–622.
- [50] N. Nagar, V. Devra, Heliyon 5 (2019), e01356.
- [51] W.Z. Tang, An Huren, Chemosphere 31 (1995) 4157–4170.
- [52] M.-C. Daniel, D. Astruc, ChemInform 35 (2004).
- [53] P.S. Sathish Kumar, R. Sivakumar, S. Anandan, J. Madhavan, P. Maruthamuthu, M. Ashokkumar, Water Res. 42 (2008) 4878–4884.
- [54] M. El-Kemary, Y. Abdel-Moneam, M. Madkour, I. El-Mehasseb, J. Lumin. 131 (2011) 570–576.
- [55] S.A. Ansari, M.M. Khan, M.O. Ansari, J. Lee, M.H. Cho, J. Phys. Chem. C 117 (2013) 27023–27030.
- [56] M.E. Khan, M.M. Khan, M.H. Cho, New J. Chem. 39 (2015) 8121–8129.
- [57] C. Grogger, S.G. Fattakhov, V.V. Jouikov, M.M. Shulaeva, V.S. Reznik, Electrochim. Acta 49 (2004) 3185–3194.
- [58] P. Christopher, H. Xin, S. Linic, Nat. Chem. 3 (2011) 467–472.
- [59] A. Kumar, M. Asthana, R. Sharma, S. Amdekar, P. Raghav, M. katoch, V.M. Katoch, Int. J. Infect. Dis. 45 (2016) 301–302.